



Article

Native Entomopathogenic Nematodes from Peru Control *Spodoptera frugiperda*, a Major Pest of *Zea mays* in the Peruvian Amazon

Grecia Fachin-Ruiz ¹, Deyvis Córdova-Sinarahua ^{2,3,4}, Lorena Estefani Romero-Chávez ¹,
Jaime Alvarado-Ramírez ¹, Cesar Quesquen-Lopez ¹¹, Eybis Flores-García ¹, Christian Koch-Duarte ³,
Agustin Cerna-Mendoza ¹, Joel Vásquez-Bardales ⁵ and Mike Corazon-Guivin ^{2,4,*}

- ¹ Laboratorio de Crianza de Insectos, Universidad Nacional de San Martín, Jr. Amorarca N° 315, Morales 22201, Peru; gvfachin@unsm.edu.pe (G.F.-R.); lorenae.rome1@gmail.com (L.E.R.-C.); jwalvarado@unsm.edu.pe (J.A.-R.); cdquesquen1@unsm.edu.pe (C.Q.-L.); ejflores@unsm.edu.pe (E.F.-G.); acerna@unsm.edu.pe (A.C.-M.)
- ² Laboratorio de Biología y Genética Molecular, Universidad Nacional de San Martín, Jr. Amorarca N° 315, Morales 22201, Peru; dcsinarahua.ppggbm@uesc.br
- ³ Estación Experimental El Porvenir, Instituto Nacional de Innovación Agraria (INIA), Carretera Marginal Sur Fernando Belaunde Terry KM 13.5, Tarapoto 22400, Peru; ckoch@inia.gob.pe
- ⁴ Centro de Biotecnología y Genética, Departamento de Ciencias Biológicas, Universidade Estadual de Santa Cruz, Rodovia Jorge Amado Km 16, Ilhéus 45662-900, Brazil
- ⁵ Faculty of Forest Sciences, National University of the Peruvian Amazon, Jr. Pevas No. 500, Iquitos 16001, Peru; joel.vasquez@unapiquitos.edu.pe
- * Correspondence: macorazon@unsm.edu.pe

Abstract

This study evaluated entomopathogenic nematodes (EPNs) isolated from a cacao agroforestry system in the Peruvian Amazon, focusing on their molecular characterization and efficacy against *Spodoptera frugiperda* (Lepidoptera: Noctuidae) larvae. Thirteen EPN isolates were obtained from 50 soil samples using the *Galleria mellonella* baiting technique. Mortality assays revealed significant differences among isolates at 24, 48, and 72 h, with isolates 11N-A4 and 8N-B1 being the most virulent, achieving maximum mortalities of 100% and 96.3% at 72 h, respectively. Median lethal time (LT₅₀) values indicated rapid action of these isolates on *G. mellonella* larvae, with 33.3 h for 11N-A4 and 32.4 h for 8N-B1. Molecular identification using ITS, D2–D3 (LSU), and COI markers confirmed the isolates as *Heterorhabditis* sp. (11N-A4) and *Heterorhabditis amazonensis* (8N-B1). In bioassays with *S. frugiperda* larvae, both EPNs exhibited dose- and time-dependent mortality. *H. amazonensis* showed rapid action, reaching 100% mortality at the highest dose (60 IJs/larvae) within 48 h, whereas *Heterorhabditis* sp. displayed a gradual, sustained increase, attaining 91% mortality at 72 h. Median lethal dose (LD₅₀) and LT₅₀ values reflected the efficiency of both isolates, with *Heterorhabditis* sp. achieving lower LD₅₀ at later stages and shorter LT₅₀ at low-to-intermediate doses. These findings highlight the potential of *Heterorhabditis* sp. and *H. amazonensis* as effective biocontrol agents adapted to local conditions and represent the first report of *H. amazonensis* in Peru. Further studies under field conditions are required to confirm their suitability for incorporation into integrated pest management strategies in the Peruvian Amazon.



Academic Editor: Francesca Barbero

Received: 22 January 2026

Revised: 19 February 2026

Accepted: 7 March 2026

Published: 9 March 2026

Copyright: © 2026 by the authors.

Licensee MDPI, Basel, Switzerland.

This article is an open access article

distributed under the terms and

conditions of the [Creative Commons](https://creativecommons.org/licenses/by/4.0/)

[Attribution \(CC BY\)](https://creativecommons.org/licenses/by/4.0/) license.

Keywords: median lethal dose LD₅₀; median lethal time LT₅₀; *Heterorhabditis amazonensis*; fall armyworm; Peruvian Amazon

1. Introduction

Maize (*Zea mays* L.) is one of the most important food crops worldwide, both for its nutritional value and its economic and social impact. It constitutes a fundamental source of food and income for millions of small- and medium-scale farmers in tropical and subtropical regions of the Americas and Asia [1,2]. However, its productivity faces several limitations, with insect pests being among the most significant. Among these pests, *Spodoptera frugiperda* [3] (Lepidoptera: Noctuidae), commonly known as the fall armyworm, is considered the most economically important [1]. This insect attacks maize from the early stages of crop development, feeding on foliage, stems, and ears, which results in severe yield losses [4–8]. Control of *S. frugiperda* has historically relied on chemical insecticides. However, intensive application has led to several problems, such as the evolution of resistant populations, a reduction in natural enemies, and adverse effects on human health and the environment [9,10]. These limitations highlight the urgent need for sustainable and environmentally friendly pest management alternatives.

Entomopathogenic nematodes (EPNs), mainly belonging to the genera *Steinernema* and *Heterorhabditis*, have emerged as effective biological control agents against a wide range of insect pests [11]. These nematodes possess a mutualistic association with symbiotic bacteria (*Xenorhabdus* spp. and *Photorhabdus* spp.), which are released into the host hemocoel after infection, causing rapid insect mortality through septicemia [11,12]. EPNs are particularly effective against soil-dwelling or cryptic insect stages, making them suitable candidates for integrated pest management programs [13]. Several species, including *Heterorhabditis bacteriophora*, *H. indica*, and *H. amazonensis*, have demonstrated high virulence against *S. frugiperda* larvae under laboratory and field conditions, supporting their potential as biological control agents in tropical agroecosystems [14–18].

Accurate identification of EPN species is essential for their effective application in biological control, as virulence, environmental adaptation, and ecological performance may vary significantly among species and even among isolates [19]. Traditionally, species identification relied on morphological and morphometric traits; however, these characteristics are often insufficient due to overlapping features and the presence of cryptic species. Consequently, molecular approaches have become fundamental for nematode taxonomy and systematics. Ribosomal DNA markers, such as the internal transcribed spacer (ITS) region and the D2–D3 expansion segments of the 28S rRNA gene, have been widely used for species identification and phylogenetic inference in the genus *Heterorhabditis* [20,21]. These markers provide valuable taxonomic information, but their resolution may be limited when distinguishing closely related or recently diverged species due to low sequence divergence [22].

To overcome these limitations, mitochondrial markers, particularly the cytochrome c oxidase subunit I (COI) gene, have been increasingly used as complementary tools for species delimitation [19,23]. The COI gene evolves faster than ribosomal markers and provides higher resolution for distinguishing closely related taxa. Advances in integrative taxonomy, combining morphological, molecular, phylogenetic, and reproductive data, have significantly improved the understanding of species boundaries within entomopathogenic nematodes. Recent studies using multilocus analyses and genomic approaches have revealed previously unrecognized diversity and clarified phylogenetic relationships within the genus *Heterorhabditis*, highlighting the importance of using multiple genetic markers for accurate species identification and evolutionary inference [19,23].

Despite these advances, the diversity and biocontrol potential of native EPNs in tropical agroforestry systems remain insufficiently explored, particularly in the Amazon region of Peru, where unique environmental conditions may harbor locally adapted and highly virulent isolates. Native isolates are especially valuable because they are better adapted to

local climatic and ecological conditions, increasing their persistence and effectiveness in the field.

Therefore, the objectives of this study were to isolate entomopathogenic nematodes from a cacao agroforestry system in the Peruvian Amazon, to identify them using molecular markers (ITS, D2–D3, and COI), and to evaluate their virulence against *Spodoptera frugiperda* larvae by determining their median lethal dose (LD₅₀) and median lethal time (LT₅₀). This integrative approach provides essential information on the taxonomy, phylogenetic placement, and biocontrol potential of native EPN isolates, contributing to the development of sustainable pest management strategies adapted to tropical agroecosystems.

2. Results

2.1. Mortality of EPNs on *Galleria mellonella*

Mortality of third-instar *G. mellonella* larvae caused by 13 different EPN isolates was compared at three evaluation times (24, 48, and 72 h) (Figure 1). Mortality differed significantly among isolates at each evaluation time ($p < 0.05$). At 24 h, isolate 11N-A4 produced the highest mortality (53.33%), followed by 8N-B1 (39.26%), both significantly higher than the other isolates, whose mortality ranged from 10.17% to 21.11%. At 48 h, mortality increased to 93.33% for 11N-A4 and 88.80% for 8N-B1, while the remaining isolates exhibited intermediate mortality levels ranging from 28.61% to 59.35%. By 72 h, isolate 11N-A4 achieved 100% mortality, and 8N-B1 reached 96.30%, whereas other isolates ranged between 37.96% and 78.52%. At all evaluation times, the control treatment exhibited the lowest mortality (<15%).

2.2. Median Lethal Time (LT₅₀) of EPNs on *G. mellonella*

LT₅₀ values for EPN isolates against third-instar *G. mellonella* larvae are presented in Table 1. Mortality caused by isolates 11N-B6, 14N-A4, and 2N-B7 and the control was <50% within 72 h post-treatment; therefore, LT₅₀ values were not calculated for these treatments. Among the evaluated isolates, 11N-A4 and 8N-B1 showed the fastest killing activity, requiring 33.3 h and 32.4 h, respectively, to reach 50% mortality. In contrast, isolates 8N-A6 (82.5 h) and 4N-A1 (86.6 h) exhibited the longest times to reach LT₅₀. Based on LT₅₀ values and high mortality levels, isolates 11N-A4 and 8N-B1 were selected as the most effective for subsequent stages of the study.

Table 1. Comparison of median lethal times (LT₅₀) in *G. mellonella* larvae for different entomopathogenic nematode (EPN) isolates.

Isolate	LT ₅₀ (h)	95% LC (h)	χ^2	<i>p</i>
11N-A3	38.5	23.7–53.3	93.1	0.0001
11N-A4	33.3	24.1–42.6	111.0	<0.0001
11N-B2	38.8	31.8–45.8	94.3	<0.0001
11N-B5	69.7	15.4–72.0	151.0	0.0578
2N-B1	51.0	31.0–71.0	92.2	0.0008
2N-B10	40.8	10.8–70.9	90.4	0.0062
4N-A1	86.6	NE	209.0	0.1660
8N-A6	82.5	NE	244.0	0.0066
8N-B1	32.4	22.2–42.7	111.0	<0.0001
8N-B3	65.4	15.9–72.0	122.0	0.0390

Note: Isolates 11N-B6, 14N-A4, and 2N-B7 and control were excluded from the table due to mortality rates below 50%. NE: Not estimated. Values in bold indicate isolates with the lowest LT₅₀ values, representing the highest virulence against *Galleria mellonella* larvae.

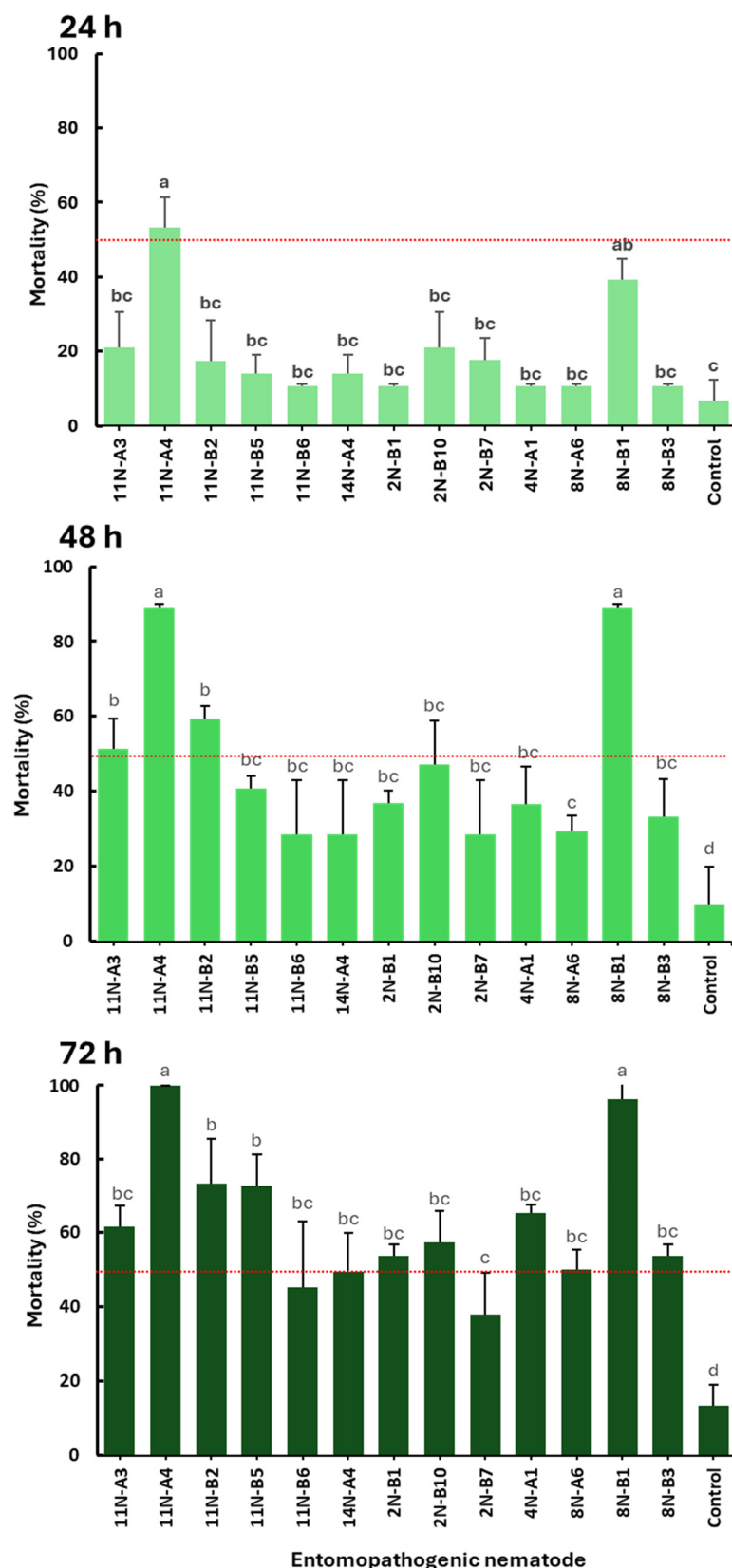


Figure 1. Mean mortality (\pm SE) of third-instar *G. mellonella* larvae exposed to 13 isolates of entomopathogenic nematodes (EPNs) at a concentration of 5 infective juveniles (IJ)/larva, evaluated at 24, 48, and 72 h post-infection. Different lowercase letters above the bars indicate significant differences among isolates at each evaluation time according to Tukey’s HSD test ($p < 0.05$). The control treatment (no EPNs) is included for comparison. The red dashed line represents the 50% mortality threshold used as a reference.

2.3. Molecular Identification of EPNs

The two isolates 11N-A4 and 8N-B1 were molecularly characterized using two nuclear markers (ITS and D2–D3) and one mitochondrial marker (COI). Edited sequences were deposited in GenBank (Supplementary Table S1). Both isolates exhibited consistent sequences across replicates, with no evidence of intraspecific variability in any of the analyzed genetic regions, indicating genomic stability in each evaluated population.

Isolate 8N-B1 showed high sequence identity with *H. amazonensis* for the ITS (99.52–99.88%) and LSU (100%) genes. Conversely, isolate 11N-A4 showed similarly high identity with *H. indica* for ITS (99.26%) and LSU (100%). For the COI gene, 11N-A4 showed 97.07% identity with *H. indica*, whereas 8N-B1 exhibited 98.40% identity with *H. amazonensis* (Figures 2–4).

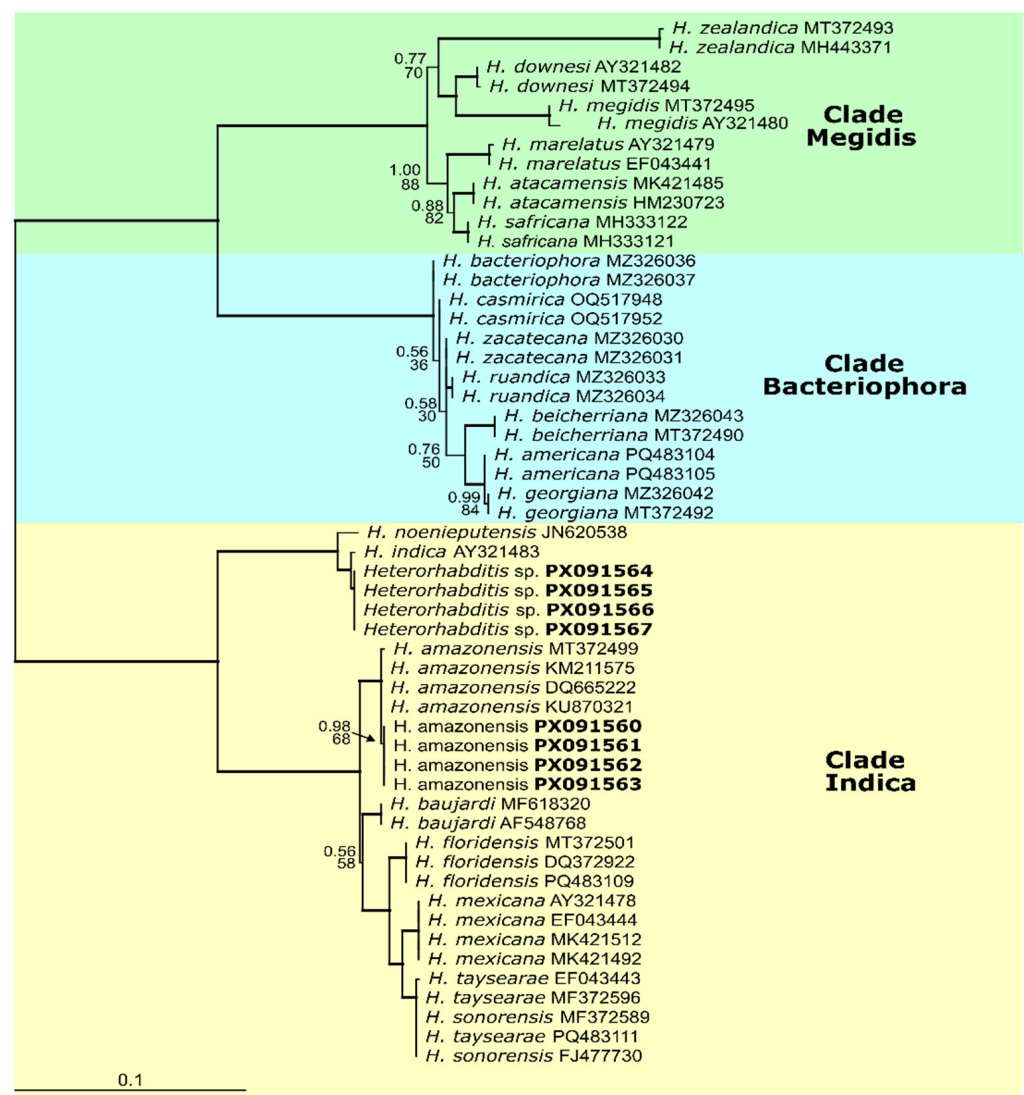


Figure 2. Phylogenetic tree obtained by analysis of ITS gene showing the relationship between the entomopathogenic nematodes isolated (in bold) and their similarity to those from GenBank. Support values (from top) are from Bayesian inference (BI) and maximum likelihood (ML). Thick branches represent clades with more than 90% support in all analyses (1000 bootstraps).

For the ITS gene (Figure 2), the dataset comprised 46 sequences from 22 previously validated species [24]. The alignment length was 800 bp, and the selected substitution model was HKY + G. Nucleotide frequencies were A = 0.252, C = 0.198, G = 0.256, and T = 0.294. The log-likelihood value was $-\ln = 3475.00$. The phylogenetic tree grouped

our isolates into two distinct clades: one corresponding to *H. amazonensis* (DQ665222, KU870321, KM211575, MT372499) and another to *H. indica* (AY321483).

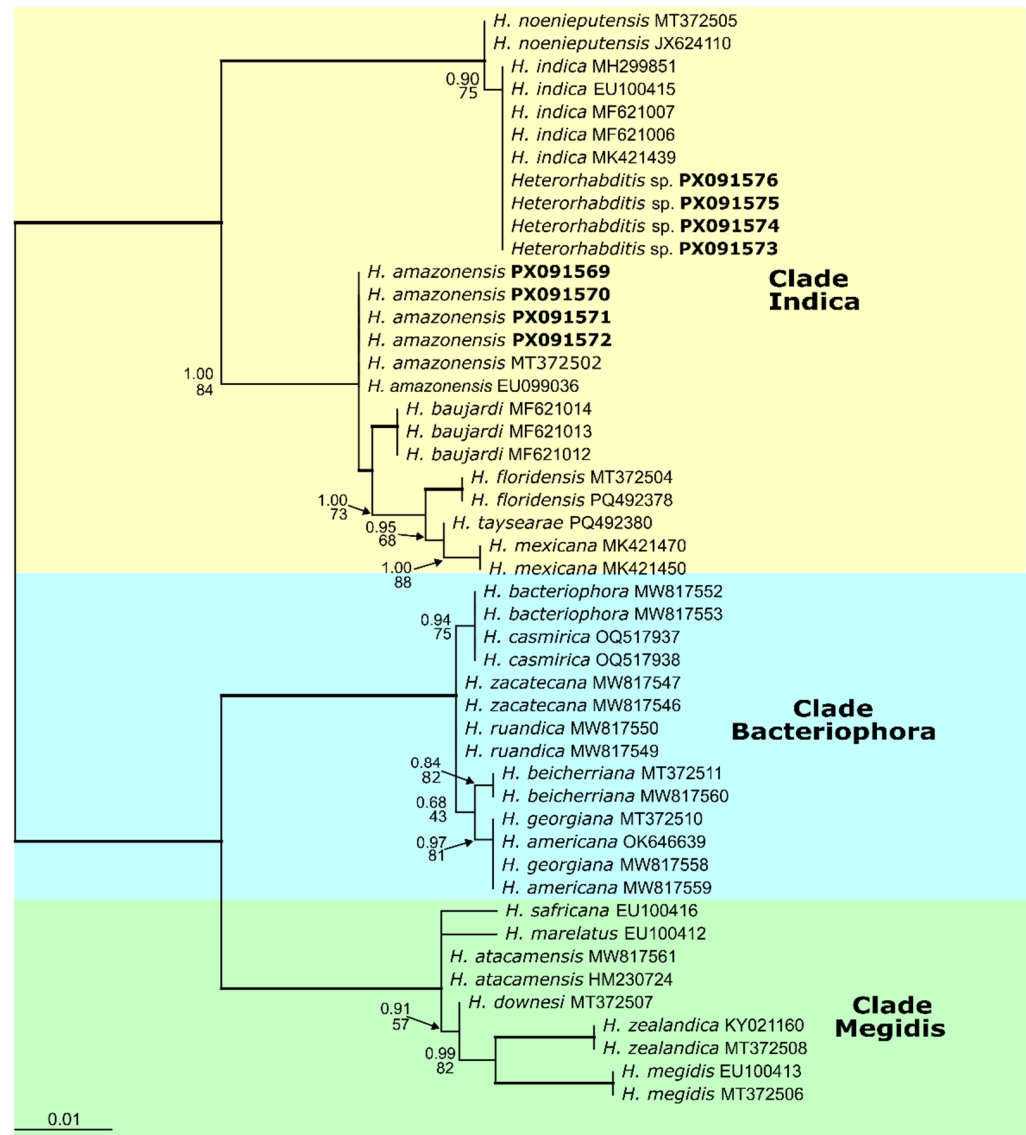


Figure 3. Phylogenetic tree obtained by analysis of D2-D3 gene showing the relationship between the entomopathogenic nematodes isolated (in bold) and their similarity to those from GenBank. Support values (from top) are from Bayesian inference (BI) and maximum likelihood (ML). Thick branches represent clades with more than 90% support in all analyses (1000 bootstraps).

For the D2–D3 LSU rRNA gene (Figure 3), the dataset included 40 sequences from 19 species, with an alignment length of 554 bp. The selected substitution model was TVMef + G, with equal nucleotide frequencies (A = 0.250, C = 0.250, G = 0.250, T = 0.250). The log-likelihood value was $-\ln = 1317.86$. The phylogenetic analysis again grouped the sequences into two clades: one corresponding to *H. amazonensis* (MT372502, EU099036) and the other to *H. indica* (MK421439, MF621006, MF621007, EU100415, MH299851).

For the COI mitochondrial gene (Figure 4), the dataset consisted of 30 sequences from 19 species, with an alignment length of 376 bp. The selected substitution model was TIM + I + G, with nucleotide frequencies A = 0.228, C = 0.089, G = 0.187, and T = 0.496. The log-likelihood value was $-\ln = 1915.68$. The resulting phylogenetic tree placed one clade within *H. amazonensis* (MT373738) and another as a distinct branch closely related to *H.*

indica (AB355853). Across all gene analyses, bootstrap and BI support values confirmed the robustness of the inferred phylogenetic relationships.

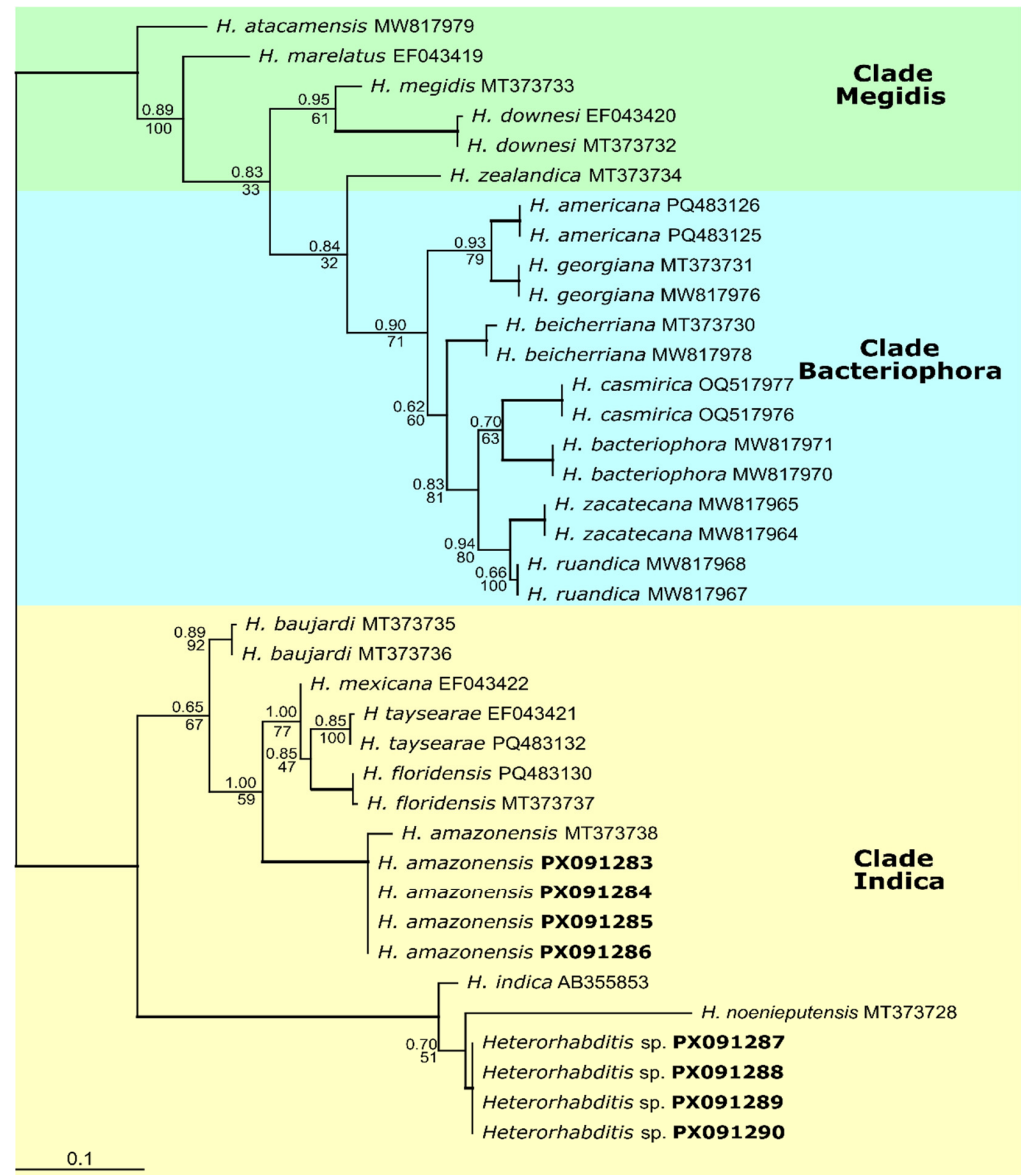


Figure 4. Phylogenetic tree obtained by analysis of COI gene showing the relationship between the entomopathogenic nematodes isolated (in bold) and their similarity to those from GenBank. Support values (from top) are from Bayesian inference (BI) and maximum likelihood (ML). Thick branches represent clades with more than 90% support in all analyses (1000 bootstraps).

2.4. Effect of EPNs on the Mortality of *S. frugiperda*

The mortality of third-instar (L3) larvae of *S. frugiperda* exposed to different concentrations and exposure times of two species of entomopathogenic nematodes (EPNs), *Heterorhabditis* sp. and *H. amazonensis*, was evaluated (Figure 5). Larval mortality of *S. frugiperda* was significantly influenced by the entomopathogenic nematode isolates (A), nematode concentration (D), and exposure time (T), as revealed by the factorial ANOVA ($p < 0.05$; Table 2). Among the evaluated factors, concentration and exposure time exhibited the strongest effects on larval mortality, with very high F values (D: $F = 2681.58$; T: $F = 3457.15$; $p = 0.001$), indicating that increases in infective juvenile concentration and longer exposure periods were key determinants of nematode efficacy.

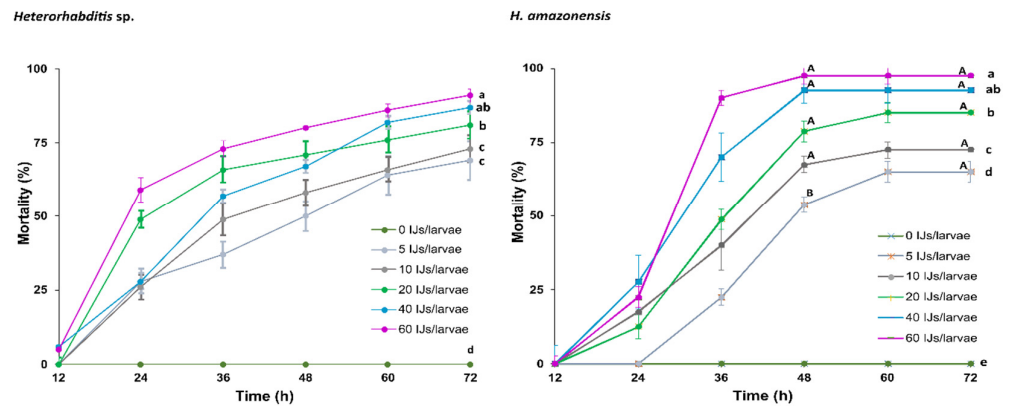


Figure 5. Corrected mortality (%) of *S. frugiperda* larvae exposed to different concentrations (5, 10, 20, 40, and 60 infective juveniles [IJs] per larva) of *Heterorhabditis* sp. and *H. amazonensis* at 12, 24, 36, 48, 60, and 72 h post-inoculation. Mortality was corrected using Abbott's formula relative to the control. Uppercase letters indicate significant differences among exposure times within the same treatment (horizontal comparisons). In contrast, lowercase letters indicate significant differences among treatments at the same exposure time (vertical comparison), according to Tukey's test ($p < 0.05$). Error bars represent the standard error of the mean (SEM).

Table 2. Analysis of variance (ANOVA) results showing the effects of entomopathogenic nematode species, concentration, exposure time, and their interactions on the mortality of *S. frugiperda* larvae.

Fuente	df	F Value	p
Isolates (A)	1	6.48	0.01 *
Dose (D)	5	2681.58	0.001 ***
Time (T)	5	3457.15	0.001 ***
A × D	5	26.52	0.001 ***
A × T	5	118.02	0.001 ***
D × T	25	163.93	0.001 ***
A × D × T	25	18.19	0.001 ***
Error	288		

Signif. codes: * $p < 0.05$; *** $p < 0.001$.

The effect of nematode isolate was also significant ($F = 6.48$; $p = 0.01$), demonstrating differences in virulence between the two isolates. Furthermore, all interaction effects ($A \times D$, $A \times T$, $D \times T$, and $A \times D \times T$) were highly significant ($p = 0.001$), indicating that larval mortality depended on the specific combination of isolate, concentration, and exposure time. These results highlight a complex interaction among the evaluated factors and support the existence of differential pathogenicity patterns and infection dynamics between the entomopathogenic nematode isolates.

For *H. amazonensis* (Figure 5), mortality remained low across all concentrations during the first 12 h post-inoculation. However, between 24 and 48 h, a sharp increase in mortality was observed at all evaluated doses. At 72 h, statistical analysis showed significant differences among treatments (60, 40, 20, 10, 5, and 0 IJs/larvae), revealing a clear dose–response relationship. Temporal comparison between 48 h and 72 h indicated that, for doses of 10, 20, 40, and 60 IJs/larvae, mortality reached its peak at 48 h and remained statistically unchanged until 72 h (capital letters). For example, the 60 IJs/larvae dose achieved 100% mortality at 48 h, while the 5 IJs/larvae dose showed a significant increase from $\approx 50\%$ at 48 h to $\approx 65\%$ at 72 h. This pattern indicates that *H. amazonensis* has a rapid mode of action, achieving high efficacy in the early stages of infection.

In the case of *Heterorhabditis* sp. (Figure 5), larval mortality showed a steady increase with both higher concentrations (IJs/larvae) and longer exposure times. During the first 12 h post-inoculation, mortality was low across all doses, reaching only 10% at the highest

dose (60 IJs/larvae). However, the mortality curve maintained an upward trend throughout the entire evaluation period, without an early plateau as seen with *H. amazonensis*. Statistical analysis at 72 h revealed significant differences among treatments (60, 40, 20, 10, 5, and 0 IJs/larvae), confirming a clear dose–response relationship. At this point, the 60 IJs/larvae dose reached approximately 91% mortality, whereas the lowest dose (5 IJs/larvae) achieved around 69%. This pattern suggests that *Heterorhabditis* sp. exhibits a more gradual mode of action, with a sustained increase in mortality over time.

At 72 h post-inoculation, the estimated median lethal dose (LD₅₀) values indicated moderate differences in virulence between the two isolates evaluated against *S. frugiperda* larvae (Table 3). *Heterorhabditis* sp. presented an LD₅₀ of 13.77 IJs/larvae (95% CI: 6.48–21.06), whereas *H. amazonensis* showed an LD₅₀ of 16.58 IJs/larvae (95% CI: 9.20–23.95). Although *Heterorhabditis* sp. required fewer infective juveniles to reach 50% mortality under these conditions, the substantial overlap of confidence intervals indicates that the differences between isolates should be interpreted with caution and do not suggest a marked divergence in virulence. The low χ^2 values (0.15 for *Heterorhabditis* sp. and 0.02 for *H. amazonensis*), together with the associated probabilities ($p = 0.58$ and $p = 0.99$, respectively), indicate an adequate fit of the probit model to the data. Overall, at 72 h post-inoculation, both isolates exhibited strong pathogenic activity against *S. frugiperda*, with comparable levels of virulence within the uncertainty range of the estimates.

Table 3. Median lethal dose (LD₅₀) of *Heterorhabditis* sp. and *H. amazonensis* at 72 h of exposure against *S. frugiperda* larvae.

Isolates	DL50 (IJs/Larvae)	95% LC	χ^2	<i>p</i>
<i>Heterorhabditis</i> sp.	13.77	6.48–21.06	0.15	0.58
<i>H. amazonensis</i>	16.58	9.20–23.95	0.02	0.99

Median lethal time (LT₅₀) values obtained for *Heterorhabditis* sp. and *H. amazonensis* revealed a clear inverse relationship between the applied dose and the time required to achieve 50% larval mortality (Table 4). In both species, increasing the dose resulted in a significant reduction in TL₅₀, indicating faster action.

Table 4. Median lethal time (LT₅₀; hours) of *Heterorhabditis* sp. and *H. amazonensis* at different doses (5, 10, 20, 40, and 60 IJs/larvae) against *S. frugiperda* larvae.

Doses (IJs/Larvae)	<i>H. amazonensis</i>				<i>Heterorhabditis</i> sp.			
	LT ₅₀ (h)	95% LC (h)	χ^2	<i>p</i>	LT ₅₀ (h)	95% LC (h)	χ^2	<i>p</i>
5	39.4	37.7–41.2	333	0.000	29.1	15.3–42.8	315	0.004
10	34.2	27.8–40.6	392	0.001	28.7	24.0–33.3	353	0.000
20	34.1	31.9–36.3	440	0.000	23.8	17.3–30.3	383	0.001
40	29.7	27.6–31.8	469	0.000	33.4	24.5–42.3	491	0.001
60	27.3	27.1–27.5	486	0.000	20.8	16.1–25.4	432	0.000

For *H. amazonensis*, the lowest dose (5 IJs/larvae) produced a LT₅₀ of 39.4 h, which progressively decreased with higher doses: 34.2 h (10 IJs/larvae), 34.1 h (20 IJs/larvae), 29.7 h (40 IJs/larvae), and 27.3 h (60 IJs/larvae), representing a total reduction of up to 12.1 h compared to the initial value. For *Heterorhabditis* sp., the TL₅₀ at 5 IJs/larvae was 29.1 h, decreasing to 28.7 h (10 IJs/larvae) and 23.8 h (20 IJs/larvae). However, at 40 IJs/larvae, there was a slight increase (33.4 h) followed by a marked decrease at the highest dose (20.8 h; 60 IJs/larvae), which was the lowest LT₅₀ recorded in the study.

Heterorhabditis sp. showed lower LT_{50} values than *H. amazonensis* at low and intermediate doses (5–20 IJs/larvae), suggesting a faster onset of action. However, at higher doses (40 IJs/larvae), *H. amazonensis* was more efficient, reaching 50% mortality earlier than *Heterorhabditis* sp.

3. Discussion

In the present study, 13 strains of native entomopathogenic nematodes (EPNs) were isolated from 50 soil samples collected in a cacao agroforestry system, representing an isolation rate of 26%. This frequency was higher than that reported in other Latin American countries, such as Chile (7%; 97 positive samples out of 1382 [25]), Colombia (0.49%; 3 out of 612 [26]), Mexico (6.6%; 4 out of 60 [27] and 4.16%; 6 out of 144 [28]), and Brazil (8%; 16 out of 201, de [29]). In these countries, isolations were carried out in conventional agricultural systems, which likely influenced the low recovery frequency of EPNs. In contrast, the isolations in our study were recovered from a cacao agroforestry system, characterized by higher plant diversity, lower soil disturbance, and more sustainable management practices. These conditions may favor both persistence and recovery of EPNs. Our results therefore highlight not only the compatibility of entomopathogens with agroecological practices but also reinforce their potential as biological control agents within integrated pest management strategies in sustainable production systems.

The 13 EPN isolates were obtained from sandy loam soils. This soil type is characterized by adequate aeration and good drainage, both of which are essential for the mobility of infective juveniles and for the development of infection processes [29–31]. These edaphic properties, together with the biodiversity of the evaluated agroforestry system, likely favor the survival and persistence of EPNs in the sampling area. Similar findings were reported by the authors of [32], who observed that EPNs were present in tropical regions with relatively high sand content, as occurred in our study (54.5% sand). Furthermore, several studies have indicated that soil pH is a determining factor in the occurrence and distribution of EPNs [33]. However, the ability of the genus *Heterorhabditis* to colonize a wide range of environments worldwide [34,35], including both conventional and organic agricultural systems [36,37], demonstrates its high ecological plasticity. This adaptability is also reflected in its frequency in sandy soils with pH values below 6 [38,39], as we observed in our study (pH 5.6).

To evaluate the pathogenicity of the 13 EPN isolates, third-instar larvae of *G. mellonella* were used as a model host. All isolates caused significant mortality, with isolates 8N-B1 and 11N-A4 showing the highest virulence, reaching 96.3% and 100% mortality at 72 h post-infection, respectively (Figure 1). Similarly, Ref. [40] reported *G. mellonella* mortality ranging from 86% to 100% at 48 h post-exposure to EPNs. These results confirm the high infectivity and virulence of the nematodes against this host, as also reported in a recent study [41].

Given their high pathogenicity, isolates 8N-B1 and 11N-A4 were selected for further experiments to assess their potential for biological control of *S. frugiperda*, an important pest of maize. Importantly, accurate taxonomic identification of highly virulent isolates is essential before considering their application in biological control programs, as cryptic species or divergent lineages within the same genus may differ in host range, environmental tolerance, and symbiotic bacterial associations.

To ensure robust identification, both isolates were characterized using nuclear (ITS and D2–D3 expansion segments of LSU rDNA) and mitochondrial (COI) markers within the genus *Heterorhabditis*. While ITS and D2–D3 are widely used in phylogenetic studies of *Heterorhabditis* [42], they are known to exhibit limited resolution among closely related taxa. In contrast, the mitochondrial cytochrome c oxidase subunit I (COI) gene is recog-

nized as a highly informative marker for species delimitation in animals due to its faster evolutionary rate and stronger discriminatory power [19,43,44].

Phylogenetic analysis based on ITS, D2–D3, and COI sequences revealed that both isolates (11N-A4 and 8N-B1) cluster within the Indica group, clearly separated from the Bacteriophora and Megidis groups. The Indica group has been subdivided into two well-supported subclades [43]: (i) the Indica subclade, including *H. indica* and *H. noenieputensis*, and (ii) the Baujardi subclade, comprising *H. amazonensis*, *H. baujardi*, *H. floridensis*, *H. mexicana*, and *H. taysearae*. Interestingly, our isolates were associated with different subclades: 11N-A4 positioned within the Indica subclade, while 8N-B1 grouped within the Baujardi subclade, in agreement with previously described evolutionary relationships (Figures 2–4).

Specifically, analyses of the nuclear markers ITS and D2–D3 placed isolate 8N-B1 within the *H. amazonensis* clade and isolate 11N-A4 within the *H. indica* clade, with sequence identity values above 99% for both genes when compared with reference sequences (Figures 2 and 3). However, mitochondrial COI analysis revealed distinct phylogenetic patterns. Isolate 11N-A4 formed an independent clade closely related to *H. indica* (sequence AB355853), showing 97.07% sequence identity. In contrast, isolate 8N-B1 clustered firmly within the *H. amazonensis* clade (MT373738), with a sequence identity of 98.40% (Figure 4).

These results are consistent with previous studies demonstrating that the nuclear ITS and D2–D3 regions provide limited resolution for discriminating closely related species within the genus *Heterorhabditis*, due to their low levels of sequence divergence. This pattern was corroborated by our phylogenetic analyses. In Figure 2 (ITS marker), the species pairs *H. sonorensis*–*H. taysearae*, *H. georgiana*–*H. americana*, and *H. ruandica*–*H. zacatecana* clustered within the same clades, indicating low interspecific differentiation with this marker. Similarly, in Figure 3 (D2–D3 marker), clustering was observed for *H. bacteriophora*–*H. casmirica*, *H. zacatecana*–*H. ruandica*, and *H. georgiana*–*H. americana*, further supporting the limited discriminatory power of nuclear ribosomal markers in recently diverged lineages. In contrast, the mitochondrial COI gene has been widely recognized as a key molecular marker for species delimitation due to its higher evolutionary rate and, consequently, greater resolving power. In *Heterorhabditis*, the interspecific differentiation threshold based on COI has been proposed to range between 97% and 98% sequence identity [44]. This criterion has been applied in the description of species such as *H. zacatecana*, *H. ruandica*, and more recently *H. americana*, where divergences within this range were considered sufficient to support their recognition as distinct species [19,44]. For instance, comparisons between *H. americana* and *H. georgiana* revealed 96.7% COI sequence identity, despite 99.8% identity in ITS and no nucleotide differences in D2–D3 [19], highlighting the limited resolving power of nuclear ribosomal markers in recently diverged taxa.

In this context, our results suggest that isolate 8N-B1 corresponds to *H. amazonensis*, as it exhibits COI identity above 98% and a phylogenetic position congruent across all three analyzed markers. In contrast, isolate 11N-A4 showed 97.07% COI identity and formed a distinct mitochondrial clade, indicating possible evolutionary divergence from *H. indica*. This divergence, which lies close to the proposed species delimitation threshold for the genus, suggests that this isolate may represent a distinct taxonomic entity. Nevertheless, in the absence of detailed morphological characterization, reproductive isolation studies, and additional multilocus analyses, we conservatively refer to this isolate as *Heterorhabditis* sp. (Unresolved taxonomic status) until further evidence allows confirmation of its taxonomic status and, potentially, its formal description as a new species.

Furthermore, these findings underscore the importance of integrating nuclear and mitochondrial markers in phylogenetic studies. While congruence among different genomic regions strengthens taxonomic assignments, incongruence, particularly involving the COI gene, may reveal relevant evolutionary processes such as recent divergence, cryptic

speciation, or population differentiation. Thus, the molecular evidence presented here not only supports the taxonomic interpretation of the studied isolates but also provides an essential evolutionary framework for understanding their biological differences, including their potential as biological control agents.

The presence of *H. amazonensis* and *Heterorhabditis* sp. in this study constitutes the first report of these species in Peru, particularly in cacao agroforestry ecosystems, thus expanding their known distribution in South America. *H. amazonensis* has previously been reported in Brazil and Venezuela [45,46], mainly in tropical and subtropical ecosystems. On the other hand, *H. indica* (a species phylogenetically close to *Heterorhabditis* sp. reported in this study) is widely recognized for its cosmopolitan distribution and high ecological tolerance. According to [47], this species has been recorded across diverse biogeographical regions: Neotropical, Nearctic, Afrotropical, Australian, Oriental, and Palearctic, with confirmed presence in Australia, Africa, Asia, North America, and South America. Its broad distribution and adaptability to different environmental conditions reinforce its potential as a biological control agent across a wide variety of agroecosystems.

Once the two isolates 11N-A4 (*Heterorhabditis* sp.) and 8N-B1 (*H. amazonensis*) were molecularly identified, their pathogenicity and virulence were tested against third-instar larvae of *S. frugiperda*. For *H. amazonensis* (8N-B1), mortality also increased in a dose-dependent manner, reaching 97% at 72 h with the highest dose (60 IJs/larvae). Comparative analysis at 72 h showed significant differences among doses (60, 40, 20, 10, 5, and 0 IJs/larvae), with doses ≥ 20 IJs/larvae resulting in significantly higher mortality compared to the lower doses (10 and 5 IJs/larvae). However, temporal analysis revealed that, for most doses, maximum mortality was reached as early as 48 h, with no significant increases thereafter for the 60, 40, 20, and 10 IJs/larvae treatments, while only the lowest dose (5 IJs/larvae) showed a significant increase between 48 h and 72 h. This pattern indicates that *H. amazonensis* exhibits a rapid mode of action, achieving high mortality levels within the first 48 h, with less temporal progression compared to *Heterorhabditis* sp., which may be related to differences in infection kinetics or the metabolic activity of its symbiotic bacterium. Although there are no previous reports evaluating this species against *S. frugiperda*, studies conducted in Brazil, where the species was originally described, highlight its pathogenic capacity against other insects. For instance, *H. amazonensis* caused 100% mortality in *G. mellonella* larvae, 85% in *Alphitobius diaperinus*, and 46% in adults of *Dichelops (Diacereus) melacanthus*, using a dose of 100 IJs/cm² [18,29].

In *Heterorhabditis* sp. (11N-A4), mortality generally followed a dose- and exposure-dependent pattern, reaching 91% at 72 h with the highest concentration (60 IJs/larvae). Analysis at 72 h revealed significant differences among treatments (60, 40, 20, 10, 5, and 0 IJs/larvae), supporting an overall dose-related response. Compared with *H. amazonensis*, *Heterorhabditis* sp. exhibited a more gradual temporal progression of mortality, suggesting a sustained mode of action rather than an abrupt lethal effect. Notably, 69% mortality was achieved at 72 h with only 5 IJs/larvae, indicating strong pathogenic potential at low infection pressure. However, quantitative comparisons of virulence parameters should be interpreted cautiously, as biological variability and overlapping confidence intervals may limit direct inference of isolate superiority. By comparison, Ref. [48] reported 100% mortality in larvae of the same stage using a substantially higher dose (250 IJs/larvae) and a lower LT₅₀ (27 h) than observed in the present study (36.10 h). Similarly, Ref. [49] obtained 75% mortality with 400 IJs/larvae of *H. indica* at 48 h post-inoculation, while Ref. [50] reported 96.07% mortality using 200 IJs/larvae of *Heterorhabditis* sp. These differences reinforce that virulence in entomopathogenic nematodes depends not only on species identity but also on isolate-specific traits, host physiological status, environmental conditions (temperature and humidity), soil characteristics, and applied dose [13,17].

At 72 h of exposure, both isolates exhibited low LD₅₀ values, reflecting high pathogenic activity. Although *Heterorhabditis* sp. required a numerically lower infective juvenile dose to achieve 50% mortality than *H. amazonensis*, the overlapping confidence intervals indicate that their virulence levels are broadly comparable. Similar inter-isolate variability has been reported in other *Heterorhabditis* species, where differences in LD₅₀ may reflect natural variation in host penetration efficiency, symbiotic bacterial virulence, and host susceptibility [14,51].

The LT₅₀ patterns generally reflected the dose-related dynamics typical of entomopathogenic nematodes. Increasing IJ density tended to reduce the time required to reach 50% mortality, although the relationship was not strictly monotonic across all treatments. In particular, the fluctuation observed at intermediate doses may be associated with biological processes such as intraspecific competition among infective juveniles, interference during host penetration, or variability in host immune responses. Similar non-linear responses have been documented in other EPN–host systems [52–54]. At low-to-intermediate doses, *Heterorhabditis* sp. tended to produce lower LT₅₀ values than *H. amazonensis*, suggesting a relatively faster onset of pathogenic activity under those conditions. At higher doses, differences between isolates were less consistent, indicating that isolate performance may vary depending on infection pressure rather than reflecting fixed superiority. Density-dependent synergistic processes, including enhanced bacterial proliferation or cooperative penetration effects, may contribute to such patterns [55,56].

Both isolates demonstrated strong pathogenic activity at the highest tested dose, consistent with previous reports identifying *Heterorhabditis* spp. as highly effective agents against lepidopteran pests, including *S. frugiperda* [16]. The ability to induce substantial mortality even at low doses supports their potential integration into IPM programs, particularly given the ecological compatibility of EPNs with other biological and cultural control strategies.

Overall, the combined LD₅₀ and LT₅₀ analyses suggest that both isolates are promising candidates for biological control applications. Rather than indicating strict superiority of one isolate over the other, the results point to complementary virulence patterns that may become advantageous under different operational conditions. Future studies assessing environmental persistence, host-seeking behavior, reproductive capacity, and field performance will be essential to determine their practical deployment potential.

Despite the promising results obtained under laboratory conditions, several limitations must be acknowledged before considering field implementation. The experiments were conducted under controlled conditions that do not fully represent the environmental variability of natural agroecosystems. Factors such as soil properties, temperature fluctuations, and ecological interactions may affect nematode survival and infectivity. Therefore, greenhouse and field evaluations are necessary to confirm their effectiveness, persistence, and suitability for integrated pest management programs.

Consistent with previous studies [57], the high pathogenic activity observed against third-instar larvae of *S. frugiperda* supports the relevance of entomopathogenic nematodes as biological control agents under diverse agricultural conditions. This study represents the first record of *H. amazonensis* in Peru and provides evidence of the biocontrol potential of both isolates against an economically important pest in the Peruvian Amazon.

4. Materials and Methods

Climatic Conditions and Soil Analysis

The cacao agroforestry system was located in a tropical dry forest (bs-T) zone, with an average annual temperature of 25.62 °C, mean relative humidity of 84.06%, and a cumulative annual precipitation of 1720 mm. Soil analysis revealed a sandy loam texture,

acidic Ph (5.78), organic matter content of 2.02%, and a bulk density of 1.45 t/m³ (Table 5). The surrounding vegetation was dominated by grasses of the genus *Brachiaria* spp.

Table 5. Physical and chemical characteristics of soil at the sampling site.

Mechanical Soil Analysis			Textural Class	pH	EC (dS/m)	OM %	N %	P ppm	K ppm	CEC
Sand %	Clay %	Silt %								
54.5	18.5	27	Sandy Loam	5.78	36.6	2.02	0.1	5.12	96.36	7.4

Culture of insects

Galleria mellonella larvae [L.] (Lepidoptera: Pyralidae) were provided by the Biomil Solutions Laboratory (Trujillo, La Libertad, Peru). Rearing was carried out in the insect rearing laboratory of the Universidad Nacional de San Martín using an artificial diet composed of wheat bran (800 g), corn flour (600 g), baker's yeast (300 g), sugar honey (1600 mL), and pollen (5 g), at 27 ± 1 °C with 70% relative humidity [58]. Last-instar *G. mellonella* larvae were used as bait insects to isolate entomopathogenic nematodes (EPNs) from soil samples and for pathogenicity assays.

S. frugiperda larvae (Lepidoptera: Noctuidae) were collected from a maize (*Zea mays*) field at the Fundo Agroforestal Aucaloma of the Universidad Nacional de San Martín, Lamas Province, San Martín, Peru (S 6°26'19.07"; W 76°25'29.76"; 720 m a.s.l.). Larvae were reared in 30 mL polypropylene cups (0.45 × 0.35 cm) containing a standard artificial diet [58] and incubated at 28 ± 1 °C with 75 ± 5% relative humidity and a 12:12 h light:dark photoperiod until the larval stage was completed. Pupae were then removed from the cups using entomological forceps and sexed under a stereomicroscope based on the morphology of the terminal abdominal segments. Virgin adults (10 males and 10 females) were placed in rearing boxes (50 × 35 × 30 cm) containing a pot with rice (*Oryza sativa*) seedlings, serving as an oviposition substrate and refuge. Egg masses were collected daily and transferred to Petri dishes; emerging larvae were fed an artificial diet [58]. When larvae reached the third instar, they were individualized in cups containing the same diet to prevent cannibalism. These F1-generation larvae were used for subsequent experiments.

Collection of soil samples

Soil samples were collected between 6:00 and 8:00 a.m. from a 1-ha *Theobroma cacao* field located in the district of Tabalosos, Lamas Province, San Martín Region, Peru (S 6°23'4.06"; W 76°38'26.60"; 641 m a.s.l.), between January and December 2021. The cacao plantation was part of an agroforestry system with *Simarouba amara*, *Swietenia mahagoni*, *Cedrela odorata*, *Citrus* sp., and *Byrsonima crassifolia*, with cacao (CCN51, Forastero and Criollo varieties) as the main crop. No chemical products were applied during crop management.

From each randomly selected cacao plant (separated by at least 5 m), three subsamples (15–20 cm depth) were collected at equidistant points around the main stem (1–2 m distance). The subsamples were combined to obtain approximately 2 kg of composite soil per plant. In total, 50 soil samples were collected, labeled, placed in polystyrene boxes, and transported to the Insect Rearing Laboratory of the Universidad Nacional de San Martín. In the laboratory, samples were processed immediately by removing stones, leaves, and roots. A portion of each sample was used for physicochemical analysis, while the remainder was used for EPN isolation. Climatic data for the field were obtained from the National Meteorology and Hydrology Service of Peru (SENAMHI–Peru) (<https://www.gob.pe/senamhi>, accessed on 4 October 2025). Surrounding vegetation at each sampling site was also recorded.

Soil Physical and Chemical Properties

Physical and chemical analyses were conducted at the Soil and Water Laboratory of the Universidad Nacional de San Martín (Tarapoto, Peru). Determined properties included soil texture, assessed using the hydrometer method [59]; pH (1:2.5 H₂O) measured with a pH meter; and electrical conductivity (1:2.5 H₂O). Available phosphorus was determined using the Olsen method [60] with spectrophotometric analysis and UV–visible reading. Additionally, available potassium and exchangeable cations (meq/100 g: Ca²⁺, Mg²⁺, K⁺, Na⁺, Al³⁺) were measured using 1N ammonium acetate (pH 7.0) followed by atomic absorption spectrophotometry. Exchangeable acidity (Al³⁺ + H⁺) was determined by titration with sodium hydroxide [61], and the cation exchange capacity (CEC) was calculated as the sum of base cations plus exchangeable acidity. Total nitrogen was determined using the Micro-Kjeldahl method [62], from which soil organic matter content was estimated.

Isolation of EPNs from soil

Entomopathogenic nematodes (EPNs) were isolated using *G. mellonella* larvae following the methodology described by [63]. Each soil sample was divided into two portions, and approximately 500 g of soil was placed in 500 mL plastic containers. Then last-instar *G. mellonella* larvae were placed on top of the soil in each container and incubated at 25 ± 2 °C for 7 days. At the end of the incubation period, cadavers showing symptoms suggestive of EPN infection were collected and placed in White traps at 25 ± 2 °C [63]. After 7 days, emerging infective juveniles (IJs) were collected, labeled, and stored in 500 mL flasks containing distilled water at 10–15 °C in a BOD incubator for a maximum of 6 days prior to use.

Production and conservation of EPNs

For culturing the different EPN isolates, stored IJs were reinoculated into last-instar *G. mellonella* larvae following the methodology of [63] with modifications. Ten *G. mellonella* larvae were placed in rectangular plastic containers (34 × 24 × 10 cm; height × width × length) lined with sterile paper towels. A suspension of approximately 1000 IJs/mL was sprayed onto the larvae using an atomizer, and larvae were incubated for 3 days to promote infection. Subsequently, infected cadavers were collected and placed in White traps [64] for 12 days. Emerging IJs were then collected and stored in sealed Ziploc bags (40 × 25 cm) containing a moist sponge (distilled water) at 10–15 °C in a BOD incubator. Only viable infective juveniles collected within 48 h were used in subsequent experimental assays.

Preliminary test

The pathogenicity and virulence of 13 entomopathogenic nematode (EPN) isolates were evaluated against those of *G. mellonella* larvae using the insect-baiting technique. Infective juveniles (IJs) were applied at a 5:1 ratio (IJs per larva), and larval mortality was recorded at 24, 48, and 72 h post-inoculation. Pathogenicity was defined as the ability to cause larval death, and virulence was quantified by median lethal time (LT₅₀). Isolates causing ≥90% mortality and exhibiting the lowest LT₅₀ values were considered highly pathogenic and virulent and selected for subsequent molecular analysis. All assays were conducted under controlled laboratory conditions and repeated three times for reproducibility.

Molecular Identification

The two EPN isolates exhibiting the highest pathogenicity (≥90% mortality) and virulence (lowest LT₅₀ values) were selected for molecular identification. The isolates were surface-sterilized following the methodology described by [65]. Genomic DNA was extracted as follows: 1.5 mL Eppendorf tubes containing surface-sterilized nematodes were supplemented with 45 µL of TE buffer (10 mM Tris-HCl; 1 mM EDTA; pH 8.0) and 5 µL of β-mercaptoethanol. Nematodes were manually homogenized using a sterile pestle. Subsequently, 450 µL of TE buffer was added, the mixture was vortexed and centrifuged at 13,000 rpm for 4 min at 4 °C, and the supernatant was discarded. The resulting pellet

was air-dried at room temperature for 30 min and resuspended in 25 μ L of ultrapure water. Extracted genomic DNA was stored at -20 °C until further use.

Polymerase chain reaction (PCR) was used to amplify three target genes/regions in the EPN isolates: the D2-D3 segment of the 28S rRNA gene (Primers: D2A-F: 5'-ACAAGTACCGTGAGGGAAAGTTG-3' and D3B-R: 5'-TCGGAAGGAACCAGCTACTA-3' [66], the ribosomal internal transcribed spacer 1 (ITS1) of the rRNA region (Primers: TW81-F: 5'-GTTTCCGTAGGTGAACCTGC-3' and AB28-R: 5'-ATATGCTTAAGTTCAGCGGGT-3' [67], and the mitochondrial cytochrome c oxidase subunit I gene (COI) (Primers: HCF-F: 5'-TTACATGATACTTATTATG-3' and HCR-R: 5'-CTGATAACTGTGACCAAATACATA-3' [68]).

PCR reactions consisted of 1 μ L of genomic DNA, 1 μ L of buffer at $10\times$, 0.2 μ L of dNTPs at 10 mM, 0.4 μ L of MgSO₄ at 50 mM, 0.04 μ L of Taq DNA Polymerase High Fidelity (Invitrogen™ Carlsbad, CA, USA) at 5 U/ μ L, 0.2 μ L of both forward and reverse primers at 10 μ M, and 10.5 μ L of dH₂O. PCR conditions included initial denaturation at 95 °C for 2 min, followed by 35 cycles at 95 °C for 30 s, 61 °C for 50 s, and 72 °C for 1 min 40 s, followed by a final extension at 72 °C for 5 min. PCR products were separated electrophoretically on 1% agarose gels, stained with Diamond™ Nucleic Acid Dye (Promega, Madison, WI, USA) and viewed by UV illumination. The bands of the expected size were excised with a scalpel. The amplified DNA was isolated from the gel with the GFX™ PCR DNA and Gel Band Purification Kit (Sigma-Aldrich, St. Louis, MO, USA) following the manufacturer's protocol, cloned into the pCR2.1 TOPO TA cloning vector (Invitrogen, Carlsbad, CA, USA) and transformed into One Shot® TOP10 chemically competent *Escherichia coli* (Invitrogen, Carlsbad, CA, USA). Four recombinant colonies of each gene/region and isolate were selected by blue/white screening and the presence of inserts detected by PCR amplification with KOD DNA Polymerase (Sigma-Aldrich, St. Louis, MO, USA) using universal forward and reverse M13 vector primers. After isolation from transformed cells, plasmids were sequenced on both strands with M13F/M13R primers using the BigDye Terminator kit 3.1v (Applied Biosystems, Foster City, CA, USA). The products were analyzed on an automated DNA sequencer (ABI 3730XL DNA analyzer—Macrogen Inc., Seoul, Republic of Korea). New sequences were deposited in GenBank.

Phylogenetic Analysis

DNA sequences were edited using MEGA X [69], and the edited sequences were submitted to BLASTn to compare them with sequences in the NCBI database (<http://blast.ncbi.nlm.nih.gov/Blast.cgi> (accessed on 4 October 2025)). From this database, highly similar sequences ($\geq 98\%$ identity for the same species) and sequences from closely related species were retrieved and included in the phylogenetic analyses (accession numbers provided in Supplementary Table S1). Three datasets were generated, D2–D3, COI and ITS. For phylogenetic reconstruction, each dataset was aligned using MAFFT v.7 [70] with default parameters.

Before phylogenetic analyses, the best-fit nucleotide substitution models for each dataset were estimated using Topali 2.5 [71]. The Transversional model with equal base frequencies and gamma distribution (TVMef + G) was applied to the D2–D3 region of the rRNA gene, the Transition model with a proportion of invariable sites and gamma distribution (TIM-I + G) was selected for the COI dataset, and the Hasegawa–Kishino–Yano model with gamma distribution (HKY + G) was used for the ITS region of the rRNA gene. These models accounted for differences in substitution rates and among-site rate heterogeneity, ensuring robust phylogenetic inference. Phylogenetic relationships were reconstructed using Bayesian inference (four runs of 1×10^6 generations, sampling frequency of 500, burn-in of 25%) and maximum likelihood analysis (1000 bootstrap replicates) in MrBayes 3.1.2 [72] and PhyML [73], respectively, executed via Topali 2.5.

Experimental Infection in *S. frugiperda*

The median lethal dose (LD₅₀) and median lethal time (LT₅₀) of two highly virulent EPN isolates (selected from the preliminary screening) were estimated against those of *S. frugiperda* larvae under controlled laboratory conditions. The experimental design corresponded to a completely randomized factorial design with three fixed factors: isolate (*Heterorhabditis* sp. and *H. amazonensis*), dose (0, 5, 10, 20, 40, and 60 infective juveniles [IJs] per larva), and time (12, 24, 36, 48, 60, and 72 h post-inoculation). The experimental unit consisted of a single healthy third-instar larva placed in a 1.5 mL Eppendorf tube containing 1 mL of sterile fine sand moistened to field capacity. Each larva was handled and maintained separately to ensure independence among experimental units. For each isolate × dose combination, five larvae were evaluated. The experiment was conducted in three independent bioassays performed at different times, each using newly prepared IJ suspensions and independent batches of larvae under identical experimental conditions. In each bioassay, mortality was recorded for every larva at 12, 24, 36, 48, 60, and 72 h post-inoculation. In total, 15 larvae were evaluated per concentration (5 larvae × 3 periods). Mortality observations at different time points were incorporated into the factorial analysis as levels of the fixed factor “time.”

Statistical Analysis

Mortality data from *G. mellonella* larvae were subjected to normality (Kolmogorov–Smirnov) and homogeneity of variance (Levene’s test) assessments. Once assumptions were met, a one-way ANOVA ($p < 0.05$) was performed using mortality values corrected with Abbott’s formula [16,48], followed by multiple comparisons using Tukey’s test ($p < 0.05$). For isolates that exceeded 50% mortality, the median lethal time (LT₅₀) was estimated for each isolate using Kaplan–Meier survival analysis [74]. The reported χ^2 statistics correspond to the goodness-of-fit of the fitted survival model for each isolate, and the associated p -values evaluate the significance of the estimated survival function. Because these statistics represent model fit rather than pairwise or global comparisons among isolates, the degrees of freedom depend on the number of observations and estimated parameters within each model.

For mortality data from *S. frugiperda* larvae, the same statistical procedure was applied, followed by estimation of the median lethal dose (LD₅₀) using Probit analysis [28]. All analyses were performed in RStudio v.4.5.1.

5. Conclusions

This study represents a significant contribution to the search for sustainable alternatives for the control of *Spodoptera frugiperda*, one of the most economically important pests in tropical agricultural systems. The molecular characterization of native entomopathogenic nematodes (EPNs) enabled the identification of two species of the genus *Heterorhabditis*, including the first record of *H. amazonensis* in the Peruvian Amazon. This finding expands current knowledge of the region’s functional biodiversity and provides valuable baseline information for future conservation, bioprospecting, and biological control initiatives.

Pathogenicity assays against third-instar larvae of *S. frugiperda* demonstrated the efficacy of both isolates, with *Heterorhabditis* sp. standing out for its higher infectivity and faster ability to induce mortality. These traits position it as a promising candidate for the development of biopesticides. However, further studies evaluating environmental tolerance, persistence, and field efficacy are required before its incorporation into integrated pest management (IPM) programs can be fully supported. The results provide a scientific foundation for future research aimed at integrating native EPNs into sustainable pest management strategies.

These traits position it as a highly promising candidate for the development of biopesticides. The results strengthen the scientific basis for incorporating EPNs into integrated

pest management (IPM) programs, contributing to reduced reliance on synthetic insecticides, mitigation of associated environmental impacts, and the promotion of more resilient, productive, and sustainable agricultural systems in the Amazon region and other tropical contexts.

Supplementary Materials: The following supporting information can be downloaded at: <https://www.mdpi.com/article/10.3390/ijms27052502/s1>.

Author Contributions: Conceptualization, G.F.-R. and M.C.-G.; methodology, G.F.-R. and L.E.R.-C.; software, C.K.-D., D.C.-S. and M.C.-G.; validation, A.C.-M., J.V.-B. and G.F.-R.; formal analysis, J.A.-R.; E.F.-G. and C.Q.-L.; investigation, G.F.-R.; data curation, C.K.-D., D.C.-S. and M.C.-G.; writing—original draft preparation, G.F.-R., C.K.-D., D.C.-S. and M.C.-G.; writing—review and editing, M.C.-G.; supervision, G.F.-R. and M.C.-G.; project administration, G.F.-R.; funding acquisition, J.A.-R. All authors have read and agreed to the published version of the manuscript.

Funding: This research was financially supported by the Research and Development Institute (IlyD) of the Universidad Nacional de San Martín for the financing of the project “Pathogenic potential of native entomopathogenic nematodes in the control of *Spodoptera frugiperda* in corn cultivation (*Zea mays* L.)” approved by Resolution N.° 594-2021-UNSM/CU-R.

Institutional Review Board Statement: Ethical review and approval were waived for this study, as it did not involve humans or vertebrate animals.

Informed Consent Statement: Not applicable.

Data Availability Statement: The datasets used and analyzed in this study are available from the corresponding author upon reasonable request.

Acknowledgments: The authors would like to thank the Universidad Nacional de San Martín (UNSM) for all its support in terms of structure and resources.

Conflicts of Interest: The authors declare no conflicts of interest.

References

1. Cázares-Sánchez, E.; Chávez-Servia, J.L.; Salinas-Moreno, Y.; Castillo-González, F.; Ramírez-Vallejo, P. Variación en la composición del grano entre poblaciones de maíz (*Zea mays* L.) nativas de Yucatán, México. *Agrociencia* **2015**, *49*, 15–30.
2. Hernández-Trejo, A.; Estrada Drouaillet, B.; Rodríguez-Herrera, R.; García Giron, J.M.; Patiño-Arellano, S.A.; Osorio-Hernández, E. Importancia del control biológico de plagas en maíz (*Zea mays* L.). *Rev. Mex. Cienc. Agrícolas* **2019**, *10*, 803–813. [\[CrossRef\]](#)
3. Smith, J.E.; Abbott, J. *The Natural History of the Rarer Lepidopterous Insects of Georgia: Including Their Systematic Characters, the Particulars of Their Several Metamorphoses, and the Plants on Which They Feed*; T. Bensley: London, UK, 1797; Volume 2, pp. 51–104.
4. Polaczyk, R.A.; da Silva, R.F.P.; Fiuza, L.M. Effectiveness of *Bacillus thuringiensis* strains against *Spodoptera frugiperda* (*Lepidoptera: Noctuidae*). *Braz. J. Microbiol.* **2000**, *31*, 165–167. [\[CrossRef\]](#)
5. Vergara, O.; Pitre, H.; Parvin, D. Economic evaluation of Lepidopterous pests in intercropped sorghum and maize in southern Honduras. *Trop. Agric.* **2001**, *78*, 190–199.
6. Rodríguez, M.R.; De León, C. El Cultivo del Maíz. In *Temas Selectos*, 1st ed.; Colegio de Posgraduados—Mundi-Prensa: Mexico City, México, 2008; pp. 29–45.
7. Oerke, E.C. Crop losses to pest. *J. Agric. Sci.* **2005**, *144*, 31–43. [\[CrossRef\]](#)
8. Ojeda-Bustamante, W.; Sifuentes-Ibarra, E.; Unland-Wess, H. Programación integral del riego en maíz en el norte de Sinaloa, México. *Agrociencia* **2006**, *40*, 13–25.
9. Huff, J.E.; Haseman, J.K. Exposure to certain pesticide may pose real carcinogenic risk. *Chem. Eng. News* **1991**, *69*, 33–37.
10. Figueroa, A.M.; Castro, E.A.; Castro, H.T. Efecto bioplaguicida de extractos vegetales para el control de *Spodoptera frugiperda* en el cultivo de maíz (*Zea mays*). *Acta Biol. Colomb.* **2019**, *24*, 58–66. [\[CrossRef\]](#)
11. Dillman, A.R.; Sternberg, P.W. Entomopathogenic nematodes. *Curr. Biol.* **2012**, *22*, R430–R431. [\[CrossRef\]](#)
12. Machado, R.A.R.; Somvanshi, V.S.; Muller, A.; Kushwah, J.; Bhat, C.G. *Photorhabdus hindustanensis* sp. nov., *Photorhabdus akhurstii* subsp. nov., and *Photorhabdus akhurstii* subsp. nov., isolated from Heterorhabditis entomopathogenic nematodes. *Int. J. Syst. Evol. Microbiol.* **2021**, *71*, 4998. [\[CrossRef\]](#)
13. Lefoulon, E.; McMullen, J.G.; Stock, S.P. Transcriptomic analysis of *Steinernema* nematodes highlights metabolic costs associated to *Xenorhabdus* endosymbiont association and rearing conditions. *Front. Physiol.* **2022**, *13*, 821845. [\[CrossRef\]](#)

14. Acharya, R.; Hwang, H.S.; Mostafiz, M.M.; Yu, Y.S.; Lee, K.Y. Susceptibility of various developmental stages of the fall armyworm, *Spodoptera frugiperda*, to entomopathogenic nematodes. *Insects* **2020**, *11*, 868. [[CrossRef](#)]
15. Kaya, H.K.; Gaugler, R. Entomopathogenic nematodes. *Ann. Rev. Entomol.* **1993**, *38*, 181–206. [[CrossRef](#)]
16. Calle, Y.H. Patogenicidad de *Heterorhabditis bacteriophora* Poinar en larvas de *Spodoptera frugiperda* en maíz. *Peruv. Agric. Res.* **2019**, *1*, 11–16. [[CrossRef](#)]
17. Kapranas, A.; Sbaiti, I.; Degen, T.; Turlings, T.C. Biological control of cabbage fly *Delia radicum* with entomopathogenic nematodes: Selecting the most effective nematode species and testing a novel application method. *Biol. Control* **2020**, *144*, 104212. [[CrossRef](#)]
18. Guide, B.A.; Andaló, V.; Ferreira, D.G.; Alves, V.S.; Fernandes, T.A.P.; Neves, P.M.O.J. First report and biological characteristics of *Heterorhabditis amazonensis* in the state of Paraná, Brazil. *Braz. J. Biol.* **2022**, *84*, e262374. [[CrossRef](#)] [[PubMed](#)]
19. Machado, R.A.R.; Abolafia, J.; Robles, M.-C.; Ruiz-Cuenca, A.N.; Bhat, A.H.; Shokoohi, E.; Půža, V.; Zhang, X.; Erb, M.; Robert, C.A.M.; et al. Description of *Heterorhabditis americana* n. sp. (*Rhabditida*, *Heterorhabditidae*), a new entomopathogenic nematode species isolated in North America. *Parasites Vectors* **2025**, *18*, 101. [[CrossRef](#)]
20. Edgington, S.; Buddie, A.G.; Moore, D.; France, A.; Merino, L.; Hunt, D.J. *Heterorhabditis atacamensis* n. sp. (*Nematoda*: *Heterorhabditidae*), a new entomopathogenic nematode from the Atacama Desert, Chile. *J. Helminthol.* **2011**, *85*, 381–394. [[CrossRef](#)]
21. Machado, R.A.R.; Bhat, A.H.; Abolafia, J.; Shokoohi, E.; Fallet, P.; Turlings, T.C.J.; Tarasco, E.; Půža, V.; Kajuga, J.; Yan, X.; et al. *Steinernema Africanum* n. sp. (*Rhabditida*, *Steinernematidae*), a New Entomopathogenic Nematode Species Isolated in the Republic of Rwanda. *J. Nematol.* **2022**, *54*, 20220049. [[CrossRef](#)]
22. Bhat, A.H.; Machado, R.A.R.; Abolafia, J.; Ruiz-Cuenca, A.N.; Askary, T.H.; Ameen, F.; Dass, W.M. Taxonomic and molecular characterization of a new entomopathogenic nematode species, *Heterorhabditis casmirica* n. sp., and whole genome sequencing of its associated bacterial symbiont. *Parasites Vectors* **2023**, *16*, 383. [[CrossRef](#)]
23. Machado, R.A.R.; Muller, A.; Hiltmann, A.; Bhat, A.H.; Půža, V.; Malan, A.P.; Castaneda-Alvarez, C.; San-Blas, E.; Duncan, L.W.; Shapiro-Ilan, D.; et al. Genome-wide analyses provide insights into genetic variation, phylo-and co-phylogenetic relationships, and biogeography of the entomopathogenic nematode genus *Heterorhabditis*. *Mol. Phylogenetics Evol.* **2025**, *204*, 108284. [[CrossRef](#)] [[PubMed](#)]
24. Půža, V.; Machado, R.A.R.; Malan, A.P. Systematics, diversity and biogeography of entomopathogenic nematodes and their bacterial symbionts. *J. Invertebr. Pathol.* **2025**, *211*, 108362. [[CrossRef](#)] [[PubMed](#)]
25. Edgington, S.; Buddie, A.G.; Moore, D.; France, A.; Merino, L.; Tymo, L.M.; Hunt, D.J. Diversity and distribution of entomopathogenic nematodes in Chile. *Nematology* **2010**, *12*, 915–928. [[CrossRef](#)]
26. Londoño-Caicedo, J.M.; Uribe-Londoño, M.; Buitrago-Bitar, M.A.; Cortés, A.J.; Muñoz-Flórez, J.E. Molecular Identification and Phylogenetic Diversity of Native Entomopathogenic Nematodes, and Their Bacterial Endosymbionts, Isolated from Banana and Plantain Crops in Western Colombia. *Agronomy* **2023**, *13*, 1373. [[CrossRef](#)]
27. Delgado-Gamboa, J.R.; Ruíz-Vega, J.; Ibarra-Rendón, J.E.; Aquino-Bolaños, T.; Giron-Pablo, S. Isolation and Identification of Native Entomopathogenic Nematodes (*Nematoda*: *Rhabditidae*) and Potential for Controlling *Scyphophorus acupunctatus* in a Laboratory. *Southwest. Entomol.* **2015**, *40*, 731–739. [[CrossRef](#)]
28. Ávila-López, M.B.; García-Maldonado, J.Q.; Estrada-Medina, H.; Hernández-Mena, D.I.; Cerqueda-García, D.; Vidal-Martínez, V.M. First record of entomopathogenic nematodes from Yucatán State, México and their infectivity capacity against *Aedes aegypti*. *PeerJ* **2021**, *9*, e11633. [[CrossRef](#)]
29. de Brida, A.; Rosa, J.; Oliveira, C.; de Castro e Castro, B.M.; Serrão, J.E.; Zanoncio, J.C.; Leite, L.G.; Wilcken, S.R.S. Entomopathogenic nematodes in agricultural areas in Brazil. *Sci. Rep.* **2017**, *7*, 45254. [[CrossRef](#)]
30. Seenivasan, N.; Prabhu, S.; Makesh, S.; Sivakumar, M. Natural occurrence of entomopathogenic nematode species (*Rhabditida*: *Steinernematidae* and *Heterorhabditidae*) in cotton fields of Tamil Nadu, India. *J. Nat. Hist.* **2012**, *46*, 2829–2843. [[CrossRef](#)]
31. El-Borai, F.E.; Stuart, R.J.; Campos-Herrera, R.; Pathak, E.; Duncan, L.W. Entomopathogenic nematodes, root weevil larvae, and dynamic interactions among soil texture, plant growth, herbivory, and predation. *J. Invertebr. Pathol.* **2012**, *109*, 134–142. [[CrossRef](#)]
32. Dolinski, C.; Kamitani, F.L.; Machado, I.R.; Winter, C.E. Molecular and morphological characterization of heterorhabditid entomopathogenic nematodes from the tropical rainforest in Brazil. *Mem. Inst. Oswaldo Cruz* **2008**, *103*, 150–159. [[CrossRef](#)]
33. Vidaurre, D.; Rodríguez, A.; Uribe, L. Factores edáficos y nemátodos entomopatógenos en un agroecosistema neotropical de banano. *Rev. Biol. Trop.* **2020**, *68*, 276–288. [[CrossRef](#)]
34. Stuart, R.J.; Barbercheck, M.E.; Grewal, P.S. Entomopathogenic Nematodes in the Soil Environment: Distributions, Interactions and the Influence of Biotic and Abiotic Factors. In *Nematode Pathogenesis of Insects and Other Pests; Sustainability in Plant and Crop Protection*; Campos-Herrera, R., Ed.; Springer: Cham, Switzerland, 2015. [[CrossRef](#)]
35. Argotti, V.E.E.; Villa, T.L.O.; Hernández, S.C.P.; Gallegos, P.; Cazar, C.M.P.; Alcazar, J. Etología de nemátodos entomopatógenos del género *Heterorhabditis* aislados de larvas de gusano blanco (*Premnotrypes vorax*) plaga de la papa (*Solanum tuberosum*) en Ecuador. *Bol. Téchnol. Ser. Zoológica* **2022**, *17*, 15–29.

36. Campos-Herrera, R.; Piedra-Buena, A.; Escuer, M.; Montalban, B.; Gutierrez, C. Effect of seasonality and agricultural practices on occurrence of entomopathogenic nematodes and soil characteristics in La Rioja (Northern Spain). *Pedobiologia* **2010**, *53*, 253–258. [[CrossRef](#)]
37. Mathios-Flores, M.A.; Pashanasi-Amasisfuén, B.; Aponte-Jaramillo, A.N.; Alcázar-Sedano, J.G.; Saire-Quispe, L.A. Aislamiento e identificación de nemátodos entomopatógenos nativos en diferentes sistemas de uso del suelo en Yurimaguas. *Rev. Peru. Investig. Agropecu.* **2022**, *1*, e9. [[CrossRef](#)]
38. Griffin, C.T.; Chaerani, R.; Fallon, D.; Reid, A.P.; Downes, M.J. Occurrence and distribution of the entomopathogenic nematodes *Steinernema* spp. and *Heterorhabditis indica* in Indonesia. *J. Helminthol.* **2000**, *74*, 143–150. [[CrossRef](#)]
39. Karabörklü, S.; Ayvaz, A.; Yilmaz, S.; Azizoglu, U.; Akbulut, M. Native entomopathogenic nematodes isolated from Turkey and their effectiveness on pine processionary moth, *Thaumetopoea wilkinsoni* Tams. *Int. J. Pest Manag.* **2014**, *61*, 3–8. [[CrossRef](#)]
40. Khashaba, E.H.K.; Moghaieb, R.E.A.; Abd El Azim, A.M.; Ibrahim, S.A.M. Isolation, identification of entomopathogenic nematodes, and preliminary study of their virulence against the great wax moth, *Galleria mellonella* L. (*Lepidoptera*: Pyralidae). *Egypt. J. Biol. Pest Control* **2020**, *30*, 55. [[CrossRef](#)]
41. Adrianzén, J.E.R.; Dávila, R.S.C.; Tesén, E.D.P.; Arias, C.P.C.; Cabrera, A.C. Ecological aspects of three strains of entomopathogenic nematodes from the department of Lambayeque-Peru. *Egypt. J. Biol. Pest Control* **2024**, *34*, 53. [[CrossRef](#)]
42. Spiridonov, S.E.; Subbotin, S.A. Phylogeny and phylogeography of *Heterorhabditis* and *Steinernema*. In *Advances in Entomopathogenic Nematode Taxonomy and Phylogeny*; Brill: Leiden, The Netherlands, 2016. [[CrossRef](#)]
43. Dhakal, M.; Nguyen, K.B.; Hunt, D.J.; Ehlers, R.-U.; Spiridonov, S.E.; Subbotin, S.A. Molecular identification, phylogeny and phylogeography of the entomopathogenic nematodes of the genus *Heterorhabditis* poinar, 1976: A multigene approach. *Nematology* **2020**, *23*, 451–466. [[CrossRef](#)]
44. Machado, R.A.R.; Bhat, A.H.; Abolafia, J.; Muller, A.; Bruno, P.; Fallet, P.; Arce, C.C.M.; Turlings, T.C.J.; Bernal, J.S.; Kajuga, J.; et al. Multi-locus phylogenetic analyses uncover species boundaries and reveal the occurrence of two new entomopathogenic nematode species, *Heterorhabditis ruandica* n. sp. and *Heterorhabditis zacatecana* n. sp. *J. Nematol.* **2021**, *53*, e2021-89. [[CrossRef](#)]
45. Andaló, V.; Nguyen, K.B.; Moino, A., Jr. *Heterorhabditis amazonensis* n. sp. (*Rhabditida*: *Heterorhabditidae*) from Amazonas. Brazil. *Nematology* **2006**, *8*, 853–867. [[CrossRef](#)]
46. Morales, N.; Morales-Montero, P.; Púza, V.; San-Blas, E. First report of *Heterorhabditis amazonensis* from Venezuela and characterization of three populations. *J. Nematol.* **2017**, *48*, 139–147. [[CrossRef](#)] [[PubMed](#)]
47. Hominick, W.M. Biogeography. In *Entomopathogenic Nematology*; CABI Publishing: Wallingford, UK, 2022; pp. 115–143. [[CrossRef](#)]
48. Abbott, W.S. A Method of Computing the Effectiveness of an Insecticide. *J. Econ. Entomol.* **1925**, *18*, 265–267. [[CrossRef](#)]
49. Shamseldean, M.S.M.; Abo-Shady, N.M.; El-Awady, M.A.M.; Heikal, M.N. *Heterorhabditis alii* n. sp. (*Nematoda*: *Heterorhabditidae*), a novel entomopathogenic nematode from Egypt used against the fall armyworm, *Spodoptera frugiperda* (Smith 1797) (*Lepidoptera*: *Noctuidae*). *Egypt. J. Biol. Pest. Control* **2024**, *34*, 13. [[CrossRef](#)]
50. Viteri, D.M.; Linares, A.M.; Flores, L. Use of the entomopathogenic nematode *Steinernema carpocapsae* in combination with low-toxicity insecticides to control fall Armyworm (*Lepidoptera*: *Noctuidae*) larvae. *Fla. Entomol.* **2018**, *101*, 327–329. [[CrossRef](#)]
51. Hazir, S.; Kaya, H.K.; Stock, S.P.; Keskin, N. *Entomopathogenic nematodes* (*Steinernematidae* and *Heterorhabditidae*) for Biological Control of Soil Pests. *Turk. J. Biol.* **2003**, *27*, 181–202.
52. Forst, S.; Clarke, D. *Bacteria-Nematode Symbiosis*; CABI Publishing: Wallingford, UK, 2002; pp. 57–77. [[CrossRef](#)]
53. Shapiro-Ilan, D.I.; Han, R.; Dolinski, C. Entomopathogenic nematode production and application technology. *J. Nematol.* **2012**, *44*, 206–217.
54. Koppenhöfer, A.M. Nematodes. In *Field Manual of Techniques in Invertebrate Pathology*, 2nd ed.; Lacey, L.A., Kaya, H.K., Eds.; Application and evaluation of pathogens for control of insects and other invertebrate pests; Springer: Berlin/Heidelberg, Germany, 2007. [[CrossRef](#)]
55. Herbert, E.E.; Goodrich-Blair, H. Friend and foe: The two faces of *Xenorhabdus nematophila*. *Nat. Rev. Microbiol.* **2007**, *5*, 634–646. [[CrossRef](#)]
56. Lacey, L.A.; Grzywacz, D.; Shapiro-Ilan, D.I.; Frutos, R.; Brownbridge, M.; Goettel, M.S. Insect pathogens as biological control agents: Back to the future. *J. Invertebr. Pathol.* **2015**, *132*, 1–41. [[CrossRef](#)]
57. Patil, J.; Linga, V.; Vijayakumar, R.; Subaharan, L.; Navik, O.; Bakthavatsalam, N.; Mhatrec, P.H.; Sekhard, J. Biocontrol potential of *Entomopathogenic nematodes* for the sustainable management of *Spodoptera frugiperda* (*Lepidoptera*: *Noctuidae*) in maize. *Pest Manag. Sci.* **2022**, *78*, 2883–2895. [[CrossRef](#)]
58. Greene, G.L.; Leppla, N.C.; Dickerson, W.A. Velvetbean Caterpillar: A Rearing Procedure and Artificial Medium. *J. Econ. Entomol.* **1976**, *69*, 487–488. [[CrossRef](#)]
59. Bouyoucos, G.J. Directions for making mechanical analyses of soils by the hydrometer method. *Soil Sci.* **1936**, *42*, 225–230. [[CrossRef](#)]
60. Chapman, H.D.; Pratt, P.F. Methods of analysis for soils, plants, and waters. *Soil Sci.* **1962**, *93*, 68. [[CrossRef](#)]

61. Yuan, T.L.; Fiskell, J.G.A. Aluminum Studies: II. The Extraction of Aluminum from Some Florida Soils†. *Soil Sci. Soc. Am. J.* **1959**, *23*, 202–205. [[CrossRef](#)]
62. Kjeldahl, J. Neue Methode zur Bestimmung des Stickstoffs in organischen Körpern. *Fresenius' Z. Anal. Chem.* **1883**, *22*, 366–382. [[CrossRef](#)]
63. Kaya, H.K.; Patricia Stock, S. Techniques in insect nematology. In *Manual of Techniques in Insect Pathology*; Academic Press: London, UK, 1997; pp. 81–324. [[CrossRef](#)]
64. White, G.F. A method for obtaining infective nematode larvae from cultures. *Science* **1927**, *66*, 302–303. [[CrossRef](#)]
65. Corazon-Guivin, M.A.; Cerna-Mendoza, A.; Guerrero-Abad, J.C.; Vallejos-Tapullima, A.; Silva, G.A.; Oehl, F. *Acaulospora aspera*, a new fungal species in the Glomeromycetes from rhizosphere soils of the inka nut (*Plukenetia volubilis* L.) in Peru. *J. Appl. Bot. Food Qual.* **2019**, *92*, 250–257. [[CrossRef](#)]
66. Subbotin, S.A.; Sturhan, D.; Chizhov, V.; Vovlas, N.; Baldwin, J.G. Phylogenetic analysis of Tylenchida Thorne, 1949 as inferred from D2 and D3 expansion fragments of the 28S rRNA gene sequences. *Nematology* **2006**, *8*, 455–474. [[CrossRef](#)]
67. Joyce, S.A.; Burnell, A.M.; Powers, T.O. Characterization of *Heterorhabditis* Isolates by PCR Amplification of Segments of mtDNA and rDNA Genes. *J. Nematol.* **1994**, *26*, 260–270.
68. Kuwata, R.; Yoshiga, T.; Yoshida, M.; Kondo, E. Phylogenetic relationships of Japanese *Heterorhabditis nematodes* and their symbiotic Photorhabdus bacteria. *Nematol. Res.* **2007**, *37*, 39–50. [[CrossRef](#)]
69. Kumar, S.; Stecher, G.; Li, M.; Knyaz, C.; Tamura, K. MEGA X: Molecular Evolutionary Genetics Analysis across Computing Platforms. *Mol. Biol. Evol.* **2018**, *35*, 1547–1549. [[CrossRef](#)] [[PubMed](#)]
70. Katoh, K.; Rozewicki, J.; Yamada, K.D. MAFFT Online Service: Multiple Sequence Alignment, Interactive Sequence Choice and Visualization. *Brief. Bioinform.* **2019**, *20*, 1160–1166. [[CrossRef](#)]
71. Milne, I.; Lindner, D.; Bayer, M.; Husmeier, D.; McGuire, G.; Marshall, D.F.; Wright, F. TOPALi v2: A Rich Graphical Interface for Evolutionary Analyses of Multiple Alignments on HPC Clusters and Multi-Core Desktops. *Bioinformatics* **2009**, *25*, 126–127. [[CrossRef](#)] [[PubMed](#)]
72. Ronquist, F.; Huelsenbeck, J.P. MrBayes 3: Bayesian Phylogenetic Inference under Mixed Models. *Bioinformatics* **2003**, *19*, 1572–1574. [[CrossRef](#)]
73. Guindon, S.; Gascuel, O. A Simple, Fast, and Accurate Algorithm to Estimate Large Phylogenies by Maximum Likelihood. *Syst. Biol.* **2003**, *52*, 696–704. [[CrossRef](#)] [[PubMed](#)]
74. Wang, A.; Fang, M.; Sun, J.; Wei, X.; Ruan, W. Investigation of Indigenous *Entomopathogenic nematodes* in Guangxi and Its Biological Control of *Spodoptera frugiperda*. *Agronomy* **2022**, *12*, 2536. [[CrossRef](#)]

Disclaimer/Publisher's Note: The statements, opinions and data contained in all publications are solely those of the individual author(s) and contributor(s) and not of MDPI and/or the editor(s). MDPI and/or the editor(s) disclaim responsibility for any injury to people or property resulting from any ideas, methods, instructions or products referred to in the content.